

Etsuko Ikeda · Kiyohito Yagi · Midori Kojima ·
Takahiro Yagyuu · Akira Ohshima · Satoshi Sobajima ·
Mika Tadokoro · Yoshihiro Katsube · Katsuhiko Isoda ·
Masuo Kondoh · Masaya Kawase · Masahiro J Go ·
Hisashi Adachi · Yukiharu Yokota · Tadaaki Kirita ·
Hajime Ohgushi

Multipotent cells from the human third molar: feasibility of cell-based therapy for liver disease

Received June 4, 2007; accepted in revised form September 17, 2007

Abstract Adult stem cells have been reported to exist in various tissues. The isolation of high-quality human stem cells that can be used for regeneration of fatal diseases from accessible resources is an important advance in stem cell research. In the present study, we identified a novel stem cell, which we named tooth germ progenitor cells (TGPCs), from discarded third molar, commonly called as wisdom teeth. We demonstrated the characterization and distinctiveness of the TGPCs, and found that TGPCs showed high proliferation activity and capability to differentiate *in vitro* into cells of three germ layers including osteoblasts, neural cells, and

hepatocytes. TGPCs were examined by the transplantation into a carbon tetrachloride (CCl₄)-treated liver injured rat to determine whether this novel cell source might be useful for cell-based therapy to treat liver diseases. The successful engraftment of the TGPCs was demonstrated by PKH26 fluorescence in the recipient's rat as to liver at 4 weeks after transplantation. The TGPCs prevented the progression of liver fibrosis in the liver of CCl₄-treated rats and contributed to the restoration of liver function, as assessed by the measurement of hepatic serum markers aspartate aminotransferase and alanine aminotransferase. Furthermore, the liver functions, observed by the levels of serum bilirubin and albumin, appeared to be improved following transplantation of TGPCs. These findings suggest that multipotent TGPCs are one of the candidates for cell-based therapy to treat liver diseases and offer unprecedented opportunities for developing therapies in treating tissue repair and regeneration.

Etsuko Ikeda¹ (✉) · Akira Ohshima · Satoshi Sobajima ·
Mika Tadokoro · Yoshihiro Katsube · Masahiro J Go ·
Hisashi Adachi · Yukiharu Yokota · Hajime Ohgushi
Research Institute for Cell Engineering (RICE)
National Institute of Advanced Industrial Science and
Technology (AIST)
3-11-46 Nakoji, Amagasaki
Hyogo 661-0974, Japan
Tel: +81 6 6494 7807
Fax: +81 6 6494 7861
E-mail: etu-ikeda@aist.go.jp

Kiyohito Yagi¹ · Midori Kojima · Katsuhiko Isoda · Masuo
Kondoh · Masaya Kawase
Graduate School of Pharmaceutical Sciences
Osaka University, Suita
Osaka 565-0871, Japan

Takahiro Yagyuu · Tadaaki Kirita
Department of Oral and Maxillofacial Surgery
Nara Medical University, Kashihara
Nara 634-8521, Japan

Key words tooth germ · multipotent · hepatocyte ·
transplantation

Introduction

The incidence of hepatocellular carcinoma (HCC) related to hepatitis C and B continues to increase in developed countries (El-Serag et al., 2003). Chronic liver injury, including that caused by virus infection, causes persistent inflammation and fibrosis, followed by the development of liver cirrhosis and HCC. Thus, the suppression of liver inflammation and/or intra-hepatic fibrogenesis could circumvent the progression to HCC.

¹Both authors are first authors.

The administration of an antiviral agent, such as interferon, can be expected to eradicate the hepatitis virus from infected patients. However, the resulting liver fibrosis is difficult to manage with drug therapy alone. Therefore, the development of an effective treatment for liver fibrosis is urgently needed for treating patients infected with hepatitis.

Recently, stem cell-based therapy has received attention as a possible alternative to organ transplantation, owing to the ability of stem cells to repopulate and differentiate at the engrafted site. Human stem cells, including embryonic stem cells (ES cells) and adult stem cells, are excellent candidates for cell-based therapy, as they can produce differentiated cells and are self-renewing. Furthermore, the enormous ability of human ES cells to differentiate into many cell types of three germ layers is encouraging (Thomson et al., 1998; Reubinoff et al., 2000). However, ethical issues and safety considerations are obstacles to clinical applications. The use of adult stem cells may circumvent the difficulties posed by ES cells, and they hold considerable clinical promise. The source of novel primitive cells that express ES cell markers such as Oct-4 and Nanog (Boyer et al., 2005) and demonstrate a perfect therapeutic effect in animal models with fatal diseases has long been awaited.

Bone marrow stem cells, including pluripotent hematopoietic stem cells (HSCs) and mesenchymal stem cells (MSCs), are thought to have great potential for cell-based therapy (Ohgushi and Caplan, 1999; Ohgushi et al., 2005). Indeed, previous studies demonstrated that bone marrow-derived MSCs can transdifferentiate into hepatocytes in rats (Petersen et al., 1999), mice (Theise et al., 2000a), and humans (Theise et al., 2000b). However, the potential plasticity of these adult stem cells remains to be clearly delineated, because many conflicting and controversial results have been reported.

Adult stem cells can be obtained from various tissues, including dental tissues (Lee et al., 2000; Toma et al., 2001; Zuk et al., 2002; Miura et al., 2003; Kogler et al., 2004; Seo et al., 2004; Yen et al., 2005). We recently showed that dental mesenchymal (dental papilla or pulp) cells from an impacted third molar germ (Fig. 1) are capable of osteogenic differentiation (Ikeda et al., 2006). Because our previous study showed the potential of exploiting the osteogenic differentiation of dental mesenchymal (dental papilla or pulp) cells in bone tissue engineering, we have further investigated the biological properties of these mesenchymal cells. We also investigated whether this possible novel source of adult stem cells might be useful for cell-based strategies to treat fatal diseases, such as liver cirrhosis and HCC. To explore the characteristics of these mesenchymal cells, we identified and characterized the clonal cell populations of dental mesenchymal (dental papilla or pulp) cells, which we call tooth germ progenitor cells (TGPCs). To investigate whether TGPCs might be useful for the treatment of liver damage, we then examined the ability

of the human TGPCs to differentiate into hepatocytes and their potential effectiveness in suppressing liver inflammation and preventing liver fibrosis in carbon tetrachloride (CCl₄)-treated rats.

Materials and methods

Harvest of dental mesenchyme

This study was approved by the ethics committee of the National Institute of Advanced Industrial Science and Technology (AIST). Partially mineralized and impacted third molar tooth germs with no eruption into the oral cavity were collected from five individuals aged 10–13 years under local anesthesia, and with written informed consent obtained from each individual and the parents of each subject. We used the dental mesenchyme of the third molar tooth germs at the late bell stage (Figs. 1C, 1F, 1G), one of the four stages of tooth development shown in Figure 1. The third molars were removed by raising soft tissue flaps for adequate exposure and removing the alveolar crest bone with high-speed surgical burs. The dental mesenchyme (dental papilla or pulp, approximately 0.4 g, Fig. 1H) was separated from the dental follicle (Fig. 1G) in the extracted third molar using forceps.

Isolation and expansion of TGPCs

The dental mesenchyme was finely minced, digested with 10 ml of 4 mg/ml collagenase (Wako, Osaka, Japan) in phosphate-buffered saline (PBS) supplemented with 1 mM CaCl₂, and shaken at 37°C for 30 min. The samples were then centrifuged at 400 × g for 10 min at 4°C to obtain a pellet, which was then suspended in maintenance medium (10 ml): Eagle's α minimal essential medium (α-MEM; Invitrogen Co., Carlsbad, CA) containing 10% fetal bovine serum (FBS; JRH Biosciences; Lenexa, KS) and the same antibiotic mixture as described previously (Ikeda et al., 2006). The cell suspension (10 ml) was placed in a 10-cm dish in the maintenance medium for primary culture. The medium was changed twice a week. During culture, cell debris and floating cells were removed, resulting in the proliferation of adherent fibroblastic cells.

At approximately 1 week, the cells became nearly confluent and were trypsinized with 0.05% trypsin and 0.53 mM EDTA. They were then seeded directly into 96-well plates at a one-cell-per-well density using the Clonocyte system of flow cytometry (FACS) Vantage (Becton Dickinson, Franklin Lakes, NJ) (passage 1). To select wells containing a single cell, the number of cells in each well was counted three times independently by different researchers. Only one cell was found in most wells, and the average colony-forming efficiency of the single cells was approximately 70%. The clonal expansion efficiency was high for all the dental mesenchyme from all five individuals. A preliminary study showed that approximately 30% of the clonal cells had *in vitro* osteogenic differentiation capability. Several growing colonies with a high proliferative activity were selected after several passages. The clonally expanded cells were trypsinized and divided into three wells of six-well plates (passage 2) for expansion. For further expansion, the cells were trypsinized and seeded at 1 × 10⁵ cells/flask in a T-75 Flask (passage 3). They were then trypsinized and suspended at a concentration of 1 × 10⁶ cells/ml in a Cell Banker (Juji Field, Tokyo, Japan) for cryopreservation at –80°C (passage 4). The cells were later thawed and seeded at 1 × 10⁵ cells/flask in a T-75 Flask for expansion. TGPCs were harvested after 7 days (passage 5) and used for differentiation assays or cell-surface analyses.

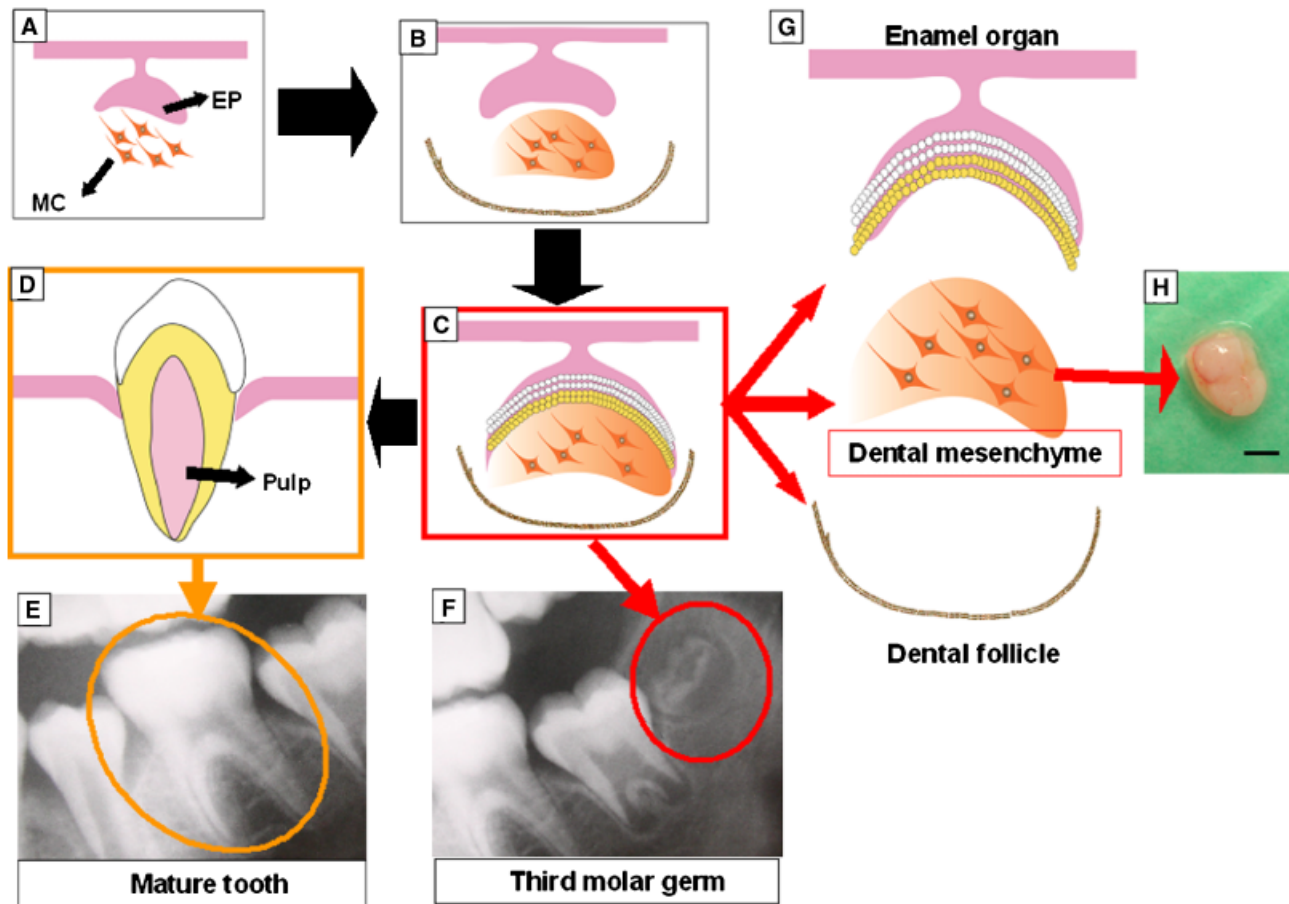


Fig. 1 Tooth development and dental mesenchyme. Bud stage; growth of epithelial cells (EP) and proliferation of mesenchymal cells (MC) (A). Cap stage; the epithelial bud enlarges into a rounded structure. MC gather and form dental mesenchyme (B). Bell stage, differentiation and calcification occur in the late bell stage. In this stage, the tooth germ consists of all three components (enamel

organ, dental mesenchyme [dental pulp or papilla], and dental follicle) (C). Tooth maturation, a mature tooth including pulp (D). Radiography of a mature tooth (E). Radiography of the tooth germ of third molar in the mandibular bone (F). Three parts of tooth germ in the late bell stage (G). Dental mesenchyme (dental pulp or papilla, H). Scale bar = 5 mm.

Preparation of TGPCs with a variant of green fluorescent protein (Venus)

For observation of TGPCs with a stable expression of Venus, a variant of GFP, we utilized a murine stem cell virus (MSCV) retroviral expression system (BD Biosciences Clontech, Palo Alto, CA). The Venus gene was generously provided by Dr. A. Miyawaki (Nagai et al., 2002). We prepared a retroviral vector pMSCV encoding Venus (Venus/pMSCV) by sub-cloning of the Venus cDNA into the pMSCVneo vector. For retroviral production, a PT67 packaging cell line was transfected with the Venus/pMSCV vector using a Fugene 6 transfection reagent (Roche Diagnostics, Basel, Switzerland) according to the manufacturer's instructions. The PT67 cells were passaged the following day in the presence of 400 $\mu\text{g}/\text{ml}$ Geneticin (G418, Invitrogen). After further culture for a couple of passages, almost all PT67 cells became positive for fluorescence from the Venus protein.

For infection of TGPCs, the PT67 cells were cultured to obtain virus-containing supernatants, and the supernatant was filtered through a 0.45- μm cellulose acetate filter. The supernatant was then supplemented with 4 $\mu\text{g}/\text{ml}$ polybrene for the final concentration (Chemicon Inc., Temecula, CA). Target TGPCs were incubated in the supernatant containing virus/polybrene overnight. The infection experiments were repeated twice at a 1-day interval. On the day following the second infection, G418 was added for a final con-

centration of 400 $\mu\text{g}/\text{ml}$ for selection. The cells were passaged twice, and Venus-transfected TGPCs were cryopreserved at -80°C . The cryopreserved TGPCs were thawed and used for *in vivo* osteogenic differentiation experiment.

In vitro osteogenic differentiation

TGPCs (passage 5) were seeded at 1×10^4 cells/well in a 12-well plate in maintenance medium. After osteogenic induction was conducted, the alkaline phosphatase (ALP) activity assay, assessment of osteocalcin content, and ALP and alizarin red S stainings were performed as described in our previous studies (Ikeda et al., 2006).

In vivo osteogenic differentiation

TGPCs (passage 5) or TGPCs transfected with Venus, (passage 6) were suspended at 1×10^6 cells/ml in the maintenance medium. Hydroxyapatite (HA) ceramic disks (CELLYARDTM; Pentax Co., Tokyo, Japan; 5 mm in diameter; 2 mm thick; pores 100 μm in diameter; an average void volume of 50%) were soaked in the TGPCs suspension at 37°C for 24 hr, and then cultured for 2 weeks under osteogenic induction to make a composite of HA with TGPCs or with TGPCs transfected with Venus as described previously (Ikeda

Table 1 Primers for reverse transcription-polymerase chain reaction

Gene	Primer sequence
Oct-4	
Forward	5'-CGACCATCTGCCGCTTTGAG-3'
Reverse	5'-CCCCCTGTCCCCATTCCT-3'
Nanog	
Forward	5'-TGCCTCACACGGAGACTGTC-3'
Reverse	5'-TGCTATTCTTCGGCCAGTTG-3'
β -actin	
Forward	5'-CCTTCCTGGGCATGGAGTC-3'
Reverse	5'-CACATCTGCTGGAAGGTGGA-3'
AFP	
Forward	5'-CTCGTTGCTTACACAAAGAAAG-3'
Reverse	5'-ATGGAAAATGAACTTGTCTATCA-3'
Albumin	
Forward	5'-TGCTTGAATGTGCTGATGACAGG-3'
Reverse	5'-AAGGCAAGTCAGCAGGCATCTCA-3'
CK18	
Forward	5'-GAGATCGAGGCTCTCAAGGA-3'
Reverse	5'-CAAGCTGGCCTTCAGATTC-3'
CK19	
Forward	5'-ATGGCCGAGCAGAACCGGAA-3'
Reverse	5'-CCATGAGCCGCTGGTACTCC-3'
Nestin	
Forward	5'-CAGCGTTGGAACAGAGGTTGG-3'
Reverse	5'-TGGCACAGGTGTCTCAAGGGTAG-3'
Tuj-1	
Forward	5'-AGATGTACGAAGACGACGAGGAG-3'
Reverse	5'-GTATCCCCGAAAATATAAACACAA-3'
Neurofilament	
Forward	5'-TGGGAAATGGCTCGTCATTT-3'
Reverse	5'-CTTCATGGAAGCGGCCAATT-3'
Human alu	
Forward	5'-CGAGGCGGGTGGATCATGAGGT-3'
Reverse	5'-TCTGTGCGCCAGGCCGACT-3'
Rat GAPDH	
Forward	5'-ATGCTGGTGTGCTGAGTATGTCG-3'
Reverse	5'-GTGGTGCAGGATGCATTGCTGA-3'

AFP, α -fetoprotein; CK18, cytokeratin18; CK19, cytokeratin19; Tuj-1, Class III β -tubulin.

et al., 2006). The composites were implanted subcutaneously in five immunocompromised animals (7-week-old male Fischer 344 rats; NJcl-rnu). The animals were sacrificed 6 weeks after implantation, and the implants with TGPCs or Venus-transfected TGPCs were harvested, fixed in 10% buffered formalin, decalcified with a chelating agent K-CX solution (Falma Co., Tokyo, Japan), and embedded in paraffin. The embedded samples were cut into sections parallel to the round surface, and stained with hematoxylin & eosin (HE). The implants with Venus-transfected TGPCs were immersed in hexane chilled in dry ice. The TGPCs-derived cells were observed with a fluorescence microscope for bone formation.

In vitro neural differentiation

TGPCs (passage 5) were seeded at 2.5×10^3 cells/well in a 12-well culture plate and cultured in α -MEM supplemented with 1% FBS, the antibiotic mixture, 50 ng/ml epidermal growth factor (EGF, PeproTech; London, UK), and 50 ng/ml platelet-derived growth factor (PDGF)-BB (R&D Systems Inc., Minneapolis, MN) for 3 days. Subsequently, the cells were cultured in α -MEM with 1% FBS, the antibiotic mixture, and 50 ng/ml basic fibroblast growth factor (bFGF, PeproTech) for 11 days, for neural differentiation.

In vitro hepatic differentiation

TGPCs (passage 5) were seeded at 5×10^3 cells/well in a collagen-coated six-well culture plate (Nitta Gelatin Inc., Osaka, Japan) for hepatic induction, which required three steps. For hepatic specification (step 1), the cells were cultured in low-glucose Dulbecco's minimal essential medium (DMEM, GIBCO, NY, USA) supplemented with 2% FBS, the antibiotic mixture, 2 mM L-glutamine (Nacalai Tesque, Kyoto, Japan), and 100 ng/ml acidic fibroblast growth factor (a-FGF, PeproTech) for 5 days. For hepatic commitment (step 2), the cells were cultured in low-glucose DMEM with 2% FBS, the antibiotic mixture, 2 mM L-glutamine, and 20 ng/ml hepatocyte growth factor (HGF, R&D Systems Inc.) for 5 days. Finally, for hepatic differentiation (step 3), the cells were cultured in low-glucose DMEM with 2% FBS, the antibiotic mixture, 2 mM L-glutamine, 20 ng/ml HGF, 10 nmol/l dexamethasone (Dex, Wako), insulin-transferrin-selenium-X (ITS-X, GIBCO), and 10 ng/ml oncostatin M (OSM, R&D Systems Inc.) for 11 days. The TGPCs were also cultured for 21 days in basal medium containing low-glucose DMEM with 2% FBS, the antibiotic mixture, and 2 mM L-glutamine as the control without hepatic induction.

In vivo hepatic differentiation

TGPCs were or were not induced to differentiate into hepatocyte-like cells (hepatic induction). After the 3-week hepatic induction, TGPCs were stained using the PKH Fluorescent Cell Linker Kit (Sigma Aldrich, St. Louis, MO) as described previously (Oyagi et al., 2006). Immunocompromised Fisher 344 rats aged 9 weeks were given an intra-peritoneal (i.p.) injection of 1 ml/kg CCl_4 in olive oil. Control animals received olive oil i.p. Two days later, 1×10^7 TGPCs were transplanted by injection into the portal vein. Sham-operated rats received a 500 μ l PBS injection. The CCl_4 treatment was performed twice a week for 4 weeks at the same dose as the first treatment, and the liver was then excised and immersed in hexane chilled in dry ice. The TGPCs-derived cells were observed with a fluorescence microscope for evidence of engraftment. The liver was harvested, and liver specimens were fixed with 10% buffered formalin and embedded in paraffin. Tissue sections were mounted on slides and stained with Azan, and the extent of fibrosis was analyzed. The fibrotic area was quantified using NIH image software. The percentage of the area showing fibrosis (blue staining) was calculated. HE staining was also performed. The blood was collected from the heart using a 21 G needle, and the serum was frozen and stored at -80°C . Serum aspartate aminotransferase (AST) and alanine aminotransferase (ALT) levels were measured using an assay kit (Transaminase CII-Test Wako, Wako). The total bilirubin and serum albumin levels were determined using an assay kit (Azwell, Osaka, Japan) and an Albumin B Test Kit (Wako), respectively. Hydroxyproline content was determined as described elsewhere (Sakaida et al., 2004).

Cell surface analysis

The cell-surface analysis of TGPCs (passage 5) was performed as described in our previous report. Fluorescein isothiocyanate (FITC)-conjugated antibodies against CD14, CD34, CD44, CD45, CD90, CD105, CD166 (Invitrogen), and CD29 (Serotec, Oxford, UK), and HLA-Class I, HLA-DR (Invitrogen), and STRO-1 (Development Study of Hybridoma Bank, DSHB, IA) were used. Mouse immunoglobulin IgG-FITC (Beckman Coulter Inc., Fullerton, CA) was used as a negative control.

Reverse transcriptase-polymerase chain reaction (RT-PCR)

Total RNA isolation and first-strand cDNA synthesis were conducted as reported previously (Ikeda et al., 2006). DNA was extracted from the liver using a TaKaRa DEXPAT™ kit (TaKaRa

Biomedicals, Kyoto, Japan). A PCR was performed using the GeneAmp PCR System 9700 (Applied Biosystems, Foster City, CA) at 94°C–96°C for 5–12 min, and 25–35 cycles at 94°C for 30 sec, 60°C–74°C for 30 sec, and 72°C for 1 min. The primer pairs used for RT-PCR analysis were designed to amplify fragments of Oct-4, Nanog, albumin, α -fetoprotein (AFP), cytokeratin 18 (CK18), cytokeratin 19 (CK19), nestin, class III β -tubulin (TuJ1), neurofilament, human *alu*, rat glyceraldehyde-3-phosphate dehydrogenase (GAPDH), and β -actin (Table 1).

Immunocytochemistry

The TGPCs were fixed with 4% paraformaldehyde (PFA) for 10 min at room temperature, treated with 0.1% Triton-X 100 (Sigma Aldrich) for 10 min, and incubated sequentially with primary monoclonal antibodies at room temperature for 4 hr. Primary antibodies against the human albumin (Cappel, West Chester, PA), TuJ1 (Covance Inc., Princeton, NJ), and nestin (Chemicon, Los Angeles, CA) were used at a dilution of 1:100. The samples were then rinsed three times with PBS and incubated for 60 min at room temperature with FITC-conjugated secondary antibodies at 1:100. Staining was visualized under an Olympus IX70 fluorescence microscope (Olympus, Tokyo, Japan).

Western blotting

The primary antibody used was against the human albumin antigen (Cappel). Western blotting analysis was carried out as reported previously (Oyagi et al., 2006).

Statistical analysis

Values are expressed as the mean and standard deviation (SD). There were two groups of continuous variables in this study. The data were analyzed for statistical significance using Dunnett's multiple comparison test, Welch's *t*-test, and Student's *t*-test. *p*-values <0.05 were considered to be statistically significant.

Results

Isolation and characterization of TGPCs

We successfully established the methods to obtain primary cultured cells from the tooth germ (Fig. 1C), which is often eliminated during the extraction of the third molar (third molar germ, Fig. 1F) at an immature stage of tooth development. Tooth development occurs from the neural crest and goes through four morphological stages including bud (Fig. 1A), cap (Fig. 1B), bell (Fig. 1C), and final maturation (Figs. 1D,1E). In this study, we used dental mesenchyme of the tooth germ in the late bell stage (Figs. 1C,1F,1G). After expansion of primary cultured cells from dental mesenchyme tissue (Fig. 1H), the deposition of single sorted cells into individual wells of 96-well plates was performed to obtain a stable and robust clonal cell line. The culture-expanded cells were tested for growth potential, and several single-cell-derived clones were selected among the clones grown. The clonal cells, TGPCs, were selected based on the exhibition of comparable growth characteristics, as shown in Figure 2A.

TGPCs were expanded and maintained for nearly 60 population doublings, during which they retained their morphology, i.e., small spindle-shaped cells with a reduced cytoplasm (Fig. 2B). Interestingly, RT-PCR analysis showed that the TGPCs expressed two transcription factors for pluripotency: Oct-4 and Nanog (Fig. 2C). These observations indicated that TGPCs have novel primitive stem cell properties because these transcription factors are involved in the regulation of cell growth and differentiation and normally restricted to pluripotent cells of the developing embryo such as epiblast cells and primordial germ cells (Boyer et al., 2005). The analysis of the cell surface by FACS demonstrated that the TGPCs were defined by expression of the following markers: CD29, CD44, CD90, CD105, CD166, and HLA-Class I. For STRO-1, TGPCs expressed at a low level. In addition, they were negative for CD14, CD34, CD45, and HLA-DR (Fig. 2D). Expression of this marker pattern was consistent in all TGPCs regardless of the donor's age or gender. The pattern of cell surface antigen expression did not vary in several TGPCs clones. Thus, the TGPCs were negative for hematopoietic markers (CD14, CD34, and CD45) but strongly positive for markers present in mesenchymal cells (CD29, CD44, CD90, CD105, and CD166) and weakly positive for STRO-1, indicating that TGPCs have a mesenchymal phenotype.

Osteogenic and neural differentiation capabilities of TGPCs

We evaluated the osteogenic differentiation potential of TGPCs cultured in the presence or in the absence of Dex. Both the ALP activity and bone-specific osteocalcin content in TGPCs with Dex (Dex+) were significantly higher than in those cultured without Dex (Dex–, Figs. 3A,3B). In addition, TGPCs cultured with Dex stained strongly with the ALP and Alizarin red S, indicating that they had the mineralizing capability of differentiated osteoblasts (Figs. 3C,3D).

Furthermore, we investigated the osteogenic differentiation potential of TGPCs *in vivo*. TGPCs were combined with HA ceramic disks and cultured to make a composite of HA with TGPCs or with TGPCs transfected with Venus, a variant of GFP. The composites were then subcutaneously implanted in immunocompromised rats. Histological sections of the HA/TGPCs implants depicted new bone formation in the pore area of the HA. Bone formation was indicated by the presence of osteocytes in the newly formed bone matrix, together with a cuboidal-shaped active osteoblast lining on the matrix surface (Fig. 3E). The analysis of the implants with Venus-transfected TGPCs showed that Venus-positive TGPCs were located within the mineralized matrix, in which osteoblasts and osteocytes were typically found (Fig. 3F).

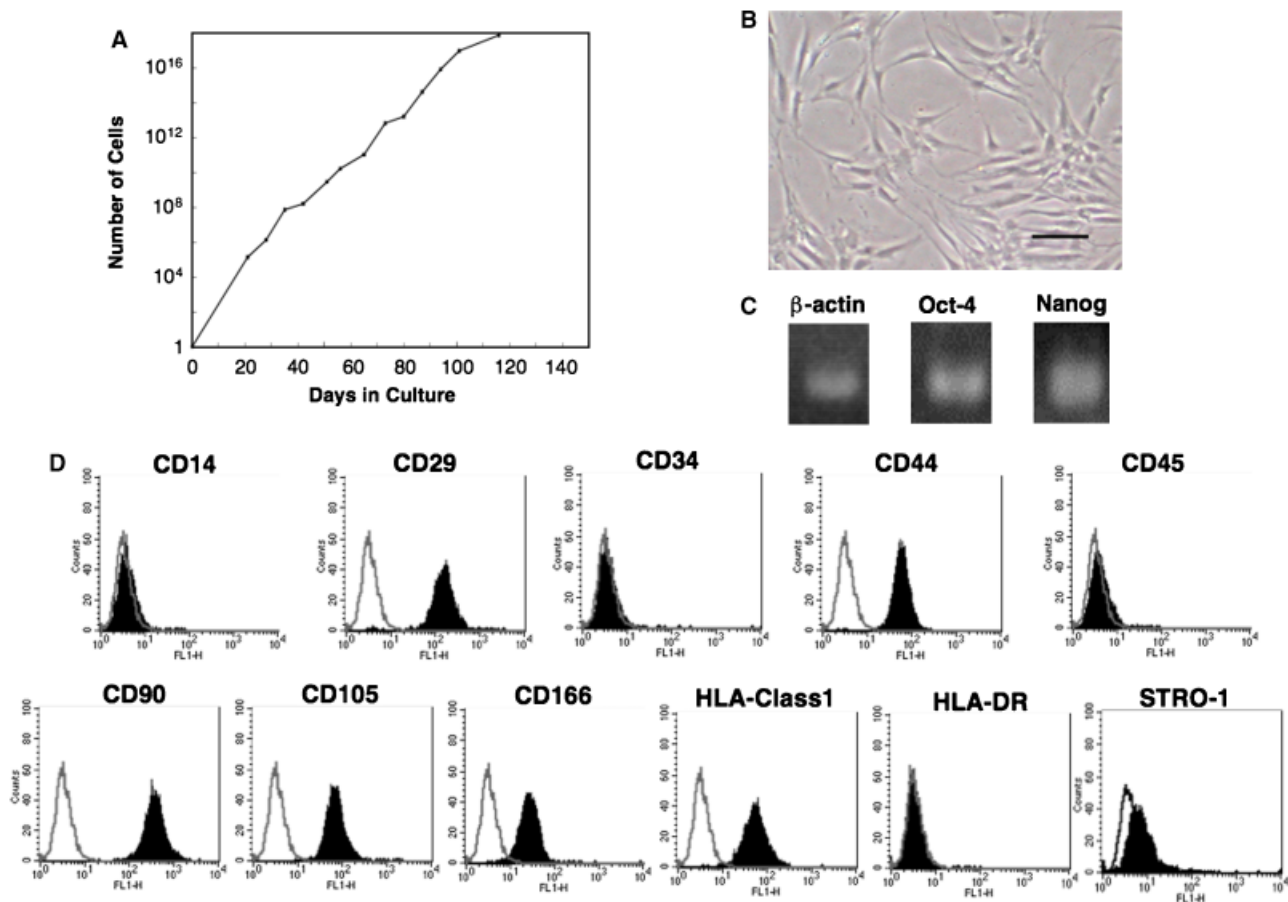


Fig. 2 Characteristics of TGPCs. Expansion in long-term culture (A). Morphology at passage 5. A homogeneous population of small spindle-shaped cells was seen (B). Scale bar = 100 μm . RT-PCR analysis for Oct-4, and Nanog (β -actin as a control, C). Cell surface analysis. Negative for CD14, CD34, CD45, and HLA-DR. Positive

for CD29, CD44, CD90, CD105, CD166, HLA-Class I, and STRO-1. Open and closed histograms stand for control immunoglobulin and specific antibody, respectively (D). TGPC, tooth germ progenitor cells; RT-PCR, reverse transcriptase-polymerase chain reaction.

To assess neural differentiation potential, neural-induced TGPCs were cultured. By 7 days after the start of neural induction, some of the cells had a neuron-like bipolar-spindle morphology. By day 14, these cells stained positive for nestin and neuron-specific TuJ1 (Figs. 3G,3H). The expression of neural-specific marker genes such as nestin, TuJ1, and neurofilament was observed by RT-PCR at different time points (Fig. 3I). After induction of neural differentiation, the mRNA expression for nestin, TuJ1, and neurofilament gradually increased with time. The results indicate that TGPCs have the potential for neural differentiation *in vitro*.

In vitro hepatic differentiation capability of TGPCs

Next, the hepatic-induced TGPCs were cultured and RT-PCR analysis was performed at different time points (Fig. 4A). RNAs for the liver-specific albumin gene, and for AFP, CK18, and CK19 were expressed to

a greater or a lesser extent during the culture period. A weak albumin mRNA signal was detected on day 10, and obvious expression was observed on days 14 and 21. In contrast, starting on day 14, the AFP and CK19 mRNA expressions gradually declined. These results indicated a certain degree of differentiation toward the phenotype of mature hepatocytes, because AFP and CK19 are typical markers of immature hepatocytes and specific biliary epithelial cells, respectively.

Albumin protein analysis was also performed at each time by Western blotting analysis (Fig. 4B), and the results were consistent with those of serial mRNA analysis of albumin. Furthermore, immunocytochemical staining for albumin at day 21 showed that hepatic-induced TGPCs were strongly positive compared with the control (non-induced) TGPCs.

These findings were consistent with the morphological changes that we observed apparently over time (Fig. 4C). The change from a bipolar-spindle and fibroblast-like to a polygonal and an epithelial-like morphology occurred in

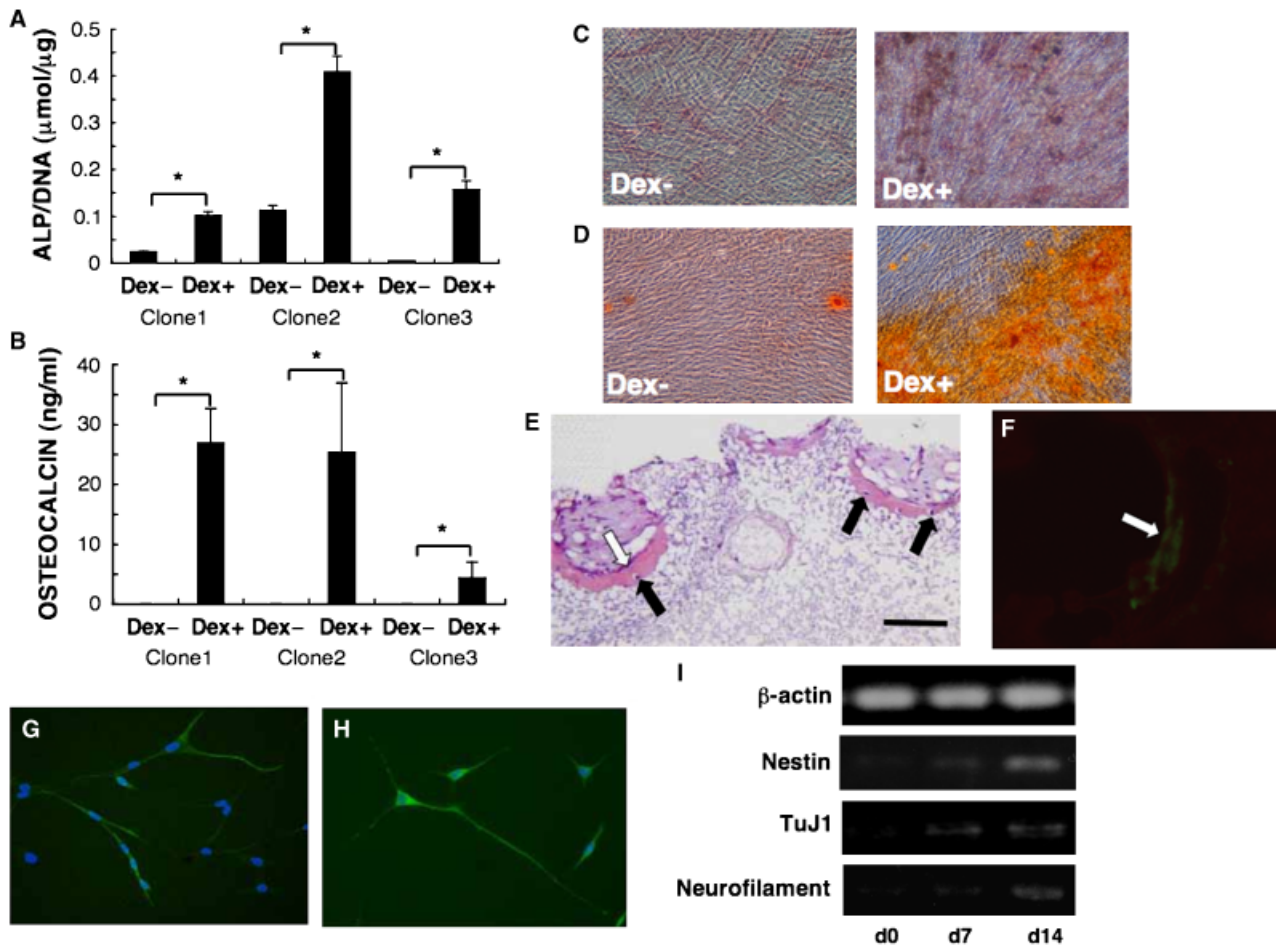


Fig. 3 Osteoblastic and neural differentiation. The ALP activity per microgram of DNA was greater in TGPCs grown with Dex (Dex+) than in those grown without Dex (Dex-) with $n = 5$ per clone. $*p < 0.05$ (A). Osteocalcin content was significantly higher in Dex+ than in Dex- cultures ($n = 5$ per clone). $*p < 0.05$ (B). ALP staining: strong ALP staining (red areas) was seen in Dex+ cultures (C). Alizarin red S staining: obvious calcium mineral deposit (red color) was seen in Dex+ cultures (D). Histological sections of HA/TGPCs composites at 8 weeks after implantation; new bone formation with osteocytes and osteoblasts was seen in the pore area of the HA. Open and black arrows represent osteoblasts and osteocytes, respectively. (HE staining, scale bar = 100 μ m, E). Anal-

ysis of implants with Venus-transfected TGPCs; Venus gene was expressed in area of new bone formation with osteocytes and osteoblasts (F). Immunocytochemical staining for nestin (G) and TuJ1 (H) in TGPCs cultured for neural induction. Neuron-like cells were observed on day 14. Bipolar-spindle-shaped cells were stained positive for nestin (G) and TuJ1 (H). Cell nuclei were stained with DAPI (G, H). Time course of RT-PCR analysis of neural markers in TGPCs 0, 7, and 14 days after neural induction (I). TGPC, tooth germ progenitor cells; RT-PCR, reverse transcriptase-polymerase chain reaction; ALP, alkaline phosphatase; HA, hydroxyapatite; HE, hematoxylin & eosin.

the TGPCs in a manner similar to the C3A cell (human-derived hepatoma cell line), a positive control. These results indicated that TGPCs can differentiate *in vitro* into cells with morphological, phenotypic, and functional characteristics of hepatocytes.

TGPCs engraftment into rats with liver injury

Given the above-mentioned findings, we investigated whether TGPCs could be useful therapeutically for the treatment of liver diseases by cell transplantation. Cultured TGPCs were transplanted *via* the portal vein into the liver of CCl₄-treated rats. The cryostat sections were

prepared to confirm the presence of transplanted TGPCs in the liver by PKH26-derived fluorescence images. As shown in Figures 5A,5B, fluorescence was observed in the liver with transplanted TGPCs. Because the stained cells formed a cluster seen in the dotted areas in the section, the transplanted TGPCs appeared to proliferate after engraftment in the liver. We further attempted to detect the human DNA-specific *alu* sequence by PCR to confirm the presence of the donor TGPCs in the rat liver (Fig. 5E). There were no amplified bands for *alu* in the DNA of sham-operated rat liver. In contrast, the bands for *alu* were seen in that of a TGPCs-transplanted rat liver.

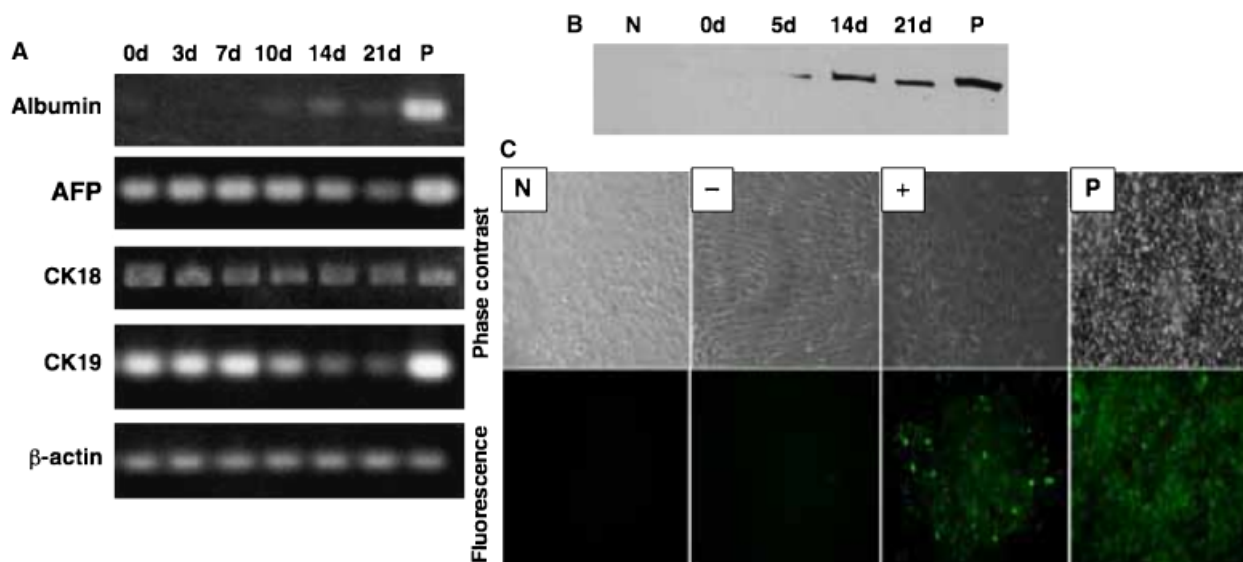


Fig. 4 *In vitro* hepatic differentiation. Time course of reverse transcriptase-polymerase chain reaction analysis of hepatic markers in TGPCs 0, 3, 7, 10, 14, and 21 days after the start of hepatic induction (A). Time course of albumin protein expression in TGPCs 0, 5, 14, and 21 days after the start of hepatic induction, by western blotting analysis (B). Immunocytochemical staining for albumin.

TGPCs cultured for hepatic induction stained positively for albumin, compared with those that were not induced to differentiate. TGPCs with (+) and without (-) hepatic induction (C). P indicates the positive control (C3A) and N indicates the negative control (fibroblasts). TGPC, tooth germ progenitor cells.

Regeneration of injured liver in rats that received transplanted TGPCs

Azan (Figs. 6A–6D) and HE (Figs. 6E–6H) stainings were performed to examine the effect of TGPCs transplantation on liver fibrosis. Following staining with Azan, a large area of fibrosis was stained blue and scattered white spots that indicated steatonecrosis were seen in the liver sections of sham-operated rats (Fig. 6B). The extents of fibrosis and steatonecrosis in the liver of CCl₄-treated rats that received transplanted TGPCs that had undergone no hepatic induction (Fig. 6C) were comparable with those in the liver of sham-operated rats (Fig. 6B). In contrast, the transplantation of the differentiated TGPCs suppressed liver fibrosis and steatonecrosis (Fig. 6D). HE staining revealed smaller areas of damage in liver sections from the recipients of hepatic induction-treated TGPCs (Fig. 6H) than in those of sham-operated animals (Fig. 6F). The effect of the TGPCs transplantation on fibrosis was evaluated by digitalization of the area stained blue by Azan (Fig. 6I). We also determined the content of liver hydroxyproline, an index of collagen content, using the method described by Sakaida et al. (2004, Fig. 6J). In agreement with the Azan staining results, the transplantation of the differentiated TGPCs significantly suppressed the hydroxyproline content.

We then used serum hepatic markers to investigate the effect of transplanted TGPCs on liver inflammation. The AST and ALT levels increased markedly to 3,333 and 732 KU, respectively, in the sham-operated rats after the CCl₄ treatment. The serum AST and ALT levels

in CCl₄-treated rats that received transplanted TGPCs that had undergone hepatic induction were significantly decreased to 972 and 239 KU, respectively. In contrast, the TGPCs cultured in the basal medium did not affect the levels significantly in CCl₄-treated rats. The serum AST and ALT levels in control animals that received olive oil were 88.9 and 13.5 KU, respectively (Figs. 6K,6L). The serum AST and ALT levels were significantly lower in CCl₄-treated recipients of hepatic induction-treated TGPCs than in sham-operated rats, and the findings indicated that the hepatic differentiation of TGPCs before transplantation into the liver was effective in suppressing liver inflammation.

The serum level of total bilirubin increased, whereas the level of albumin decreased after the CCl₄ treatment in the control rats. The transplantation of the differentiated TGPCs reduced both the increase in bilirubin and the suppression of albumin (Figs. 6M,6N).

Discussion

In this study, we characterized clonally expanded TGPCs in terms of their morphology, proliferation, and multipotency. *In vitro*, TGPCs had a mesenchymal phenotype, were self-renewing, and differentiated into cells of three germ layers. Furthermore, transplanted human TGPCs that had undergone hepatic induction survived, and the recipient CCl₄-treated rats showed less injury to the liver than the control animals, suggesting that TGPCs might have clinical applications.

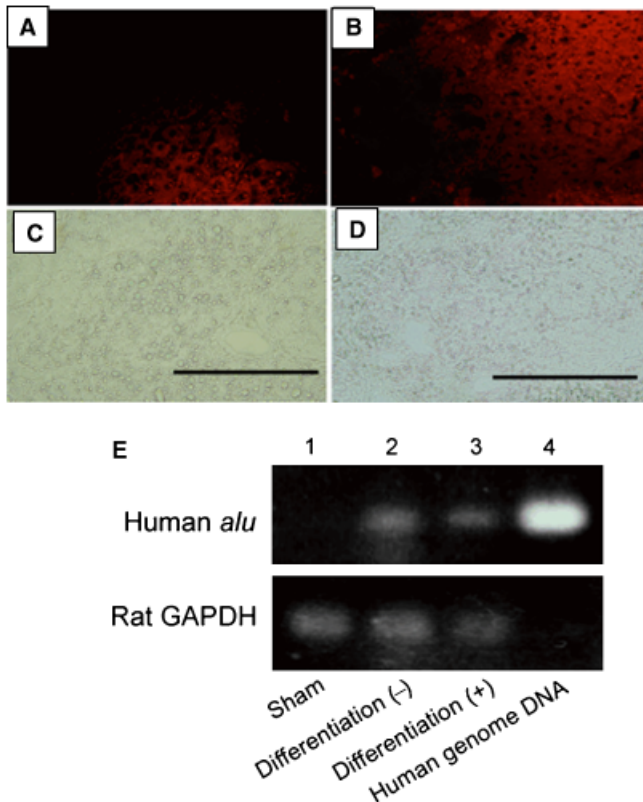


Fig. 5 Transplantation of TGPCs into CCl₄-injured rat liver. Engraftment of TGPCs. Liver sections post transplantation of PKH-26 stained TGPCs cultured without (A and C) or with (B and D) hepatic induction. Fluorescence (Upper, A and B) and bright-field (Lower, C and D) images are shown (Scale bars = 100 μ m, A–D). Polymerase chain reaction analysis was performed using primers for human *alu* and rat GAPDH. DNA was isolated from the liver of sham-operated rats (Sham) and of rats after the transplantation of TGPCs with and without hepatic induction (Differentiation (+) and Differentiation (–), respectively). Human genome DNA was the positive control (E). TGPC, tooth germ progenitor cells; GAPDH, glyceraldehyde-3-phosphate dehydrogenase; CCl₄, carbon tetrachloride.

Previously, another group showed that clonal cells from the bone marrow differentiate *in vitro* into cells of all three germ layers (Zipori, 2005). Likewise, D’Ippolito et al. (2004) described the same *in vitro* potential for bone marrow-derived adult multilineage inducible (MIAMI) cells. Like MIAMI and other cells that are described in the aforementioned reports (D’Ippolito et al., 2004; Zipori, 2005), TGPCs are thought to be very primitive cells as they showed multilineage differentiation and proliferation capabilities and expressed transcriptional factors associated with pluripotency: Oct-4 and Nanog (Fig. 2).

It has been reported recently that multipotent cells can be isolated from dental tissues such as the dental pulp and dental ligament (Miura et al., 2003; Seo et al., 2004). Iohara et al. (2006) reported that side population cells from porcine dental pulp have the potential for dentinogenesis, chondrogenesis, adipogenesis, and neurogenesis. In these reports, the characterization of

clonal cells and the differentiation potential into the endodermal lineage have not been mentioned. Here, this may be the first report that explains the characterization of clonal cells that have greater multipotency than those dental stem cells reported previously and can be obtained from human dental tissues that are discarded during dental treatment. Also, this study provides the first evidence that the stem cells from the neural crest-derived dental tissue can give rise to endoderm cell lineages such as hepatocytes.

Recently, sources of adult stem cells besides the bone marrow, including adipose tissue, term placenta, and placental and/or umbilical cord blood, have been reported. These cells have the potential to differentiate into cell types belonging to tissues besides their tissue of origin (Zuk et al., 2002; Kogler et al., 2004; Yen et al., 2005). For example, and with regard to hepatic differentiation, Seo et al. (2005) reported that human adipose tissue-derived stromal cells transplanted into CCl₄-injured SCID (severe combined immunodeficiency) mice differentiate into hepatocytes *in vivo*. Another recent report demonstrated that umbilical cord blood stem cells differentiate into hepatocytes after transplantation into CCl₄-injured rats (Tang et al., 2006). However, these reports did not address the therapeutic effects of these cells.

We and other groups successfully demonstrated that CCl₄-induced liver fibrosis was suppressed following the transplantation of bone marrow-derived MSCs into rats (Oyagi et al., 2006) and mice (Sakaida et al., 2004). Importantly, in the present study, we succeeded in cloning multipotent adult progenitor cells (TGPCs) from the human tooth germ, and showed that TGPCs that were subjected to *in vitro* hepatic induction had a significant therapeutic effect on CCl₄-induced liver injury (Fig. 4). Following clonal expansion, differentiated TGPCs suppressed inflammation and fibrosis in the liver of CCl₄-treated rats and contributed to the restoration of liver function, as assessed by the measurement of hepatic serum markers (Fig. 6). Thus, the extensive proliferation and differentiation capabilities of TGPCs are promising in terms of them being an accessible source for liver tissue engineering approaches.

Our data showed that novel multipotent progenitor cells, TGPCs, might have greater potential for proliferation than the “gold standard” bone marrow MSCs. Furthermore, taking into account the durable viability of cryopreserved TGPCs, it is possible that such cells could be frozen and used later, as needed, in regenerative medicine for autograft, once the cell banking system has been established. Based on the results of our previous study (Akahane et al., 1999), in which allogeneic MSCs survived *in vivo* with appropriate immunosuppressant treatment, we postulate that allogeneic TGPCs given with immunosuppressants or human leukocyte antigen-matched donor TGPCs may be useful for novel tissue engineering therapies. These

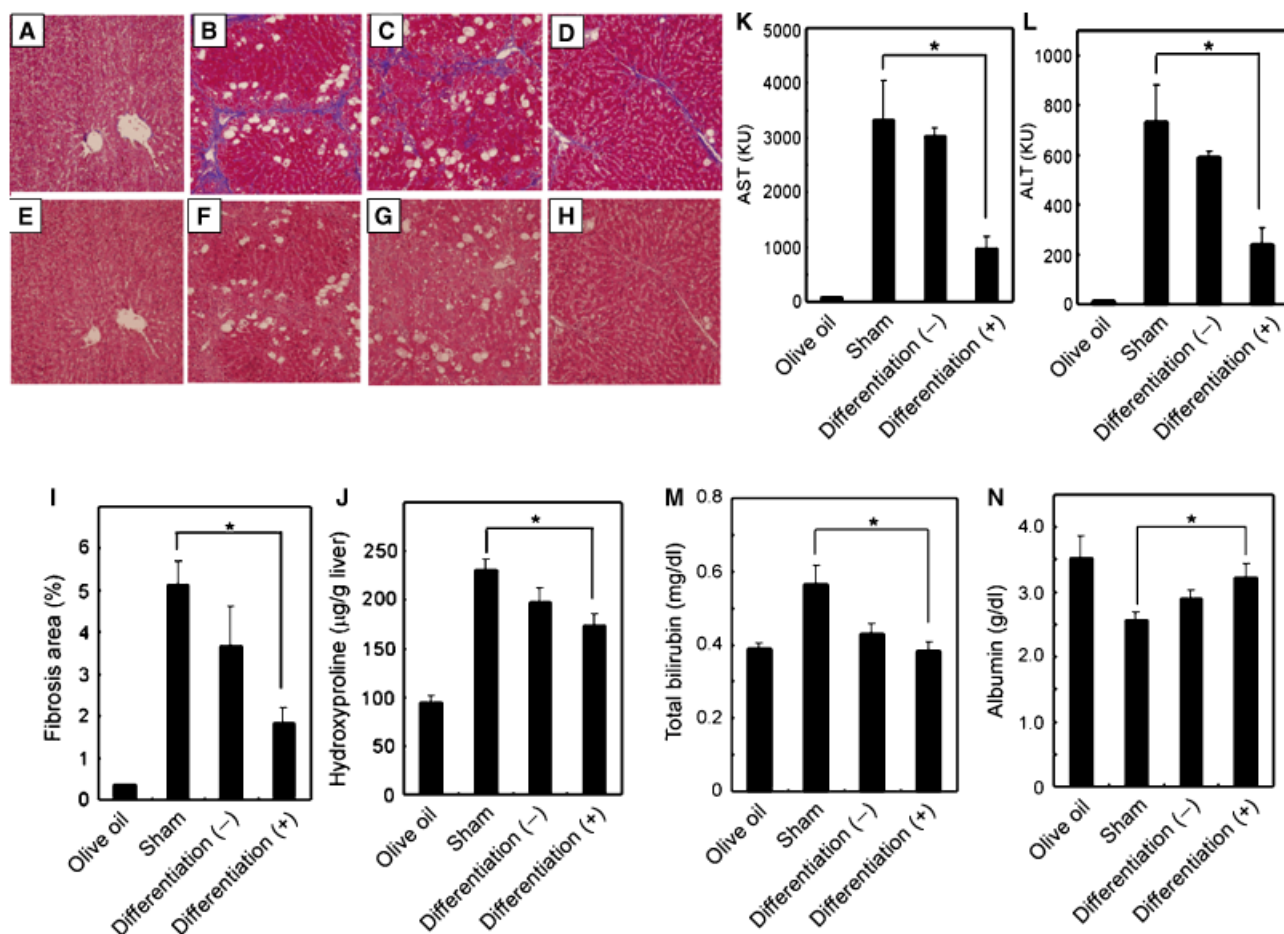


Fig. 6 Suppression of fibrosis and recovery of liver function. Liver sections after staining with Azan (A–D) and HE (E–H). The CCl₄-injured liver of sham-operated rats (Sham, B and F) and of animals that received transplanted TGPCs with or without hepatic induction (differentiation [+], D and H; differentiation [–], C and G), and the liver of the control animals that received olive oil (Olive oil, A and E). Quantification of liver fibrosis in the CCl₄-injured rat liver. The fibrotic area was calculated for five randomly selected liver sections per rat (I). Hydroxyproline content in the liver (J). AST and ALT levels in rat livers in groups Sham, differentiation (+), and differentiation (–). A significant difference was seen be-

tween the values in the Sham ($n = 4$) and differentiation (+) ($n = 3$) groups. KU stands for Karmen unit (K and L). The total bilirubin (M) and serum albumin level (N). The findings indicate the recovery of liver functions in CCl₄-injured livers harboring transplanted TGPCs with hepatic differentiation. Values are means \pm SD for individual animals. A significant difference was seen between the values in the Sham and differentiation (+) groups. * $p < 0.05$. TGPC, tooth germ progenitor cells; CCl₄, carbon tetrachloride; AST, aspartate aminotransferase; ALT, alanine aminotransferase; HE, hematoxylin & eosin.

promising strategies of ours including transplantation of novel multipotent TGPCs could help halt malignant progression to HCC in hepatitis patients receiving antiviral treatment. In the future, the surprising potential of TGPCs we evidenced *in vivo* may create new avenues for cell-based therapy to treat other fatal diseases.

References

- Akahane, M., Ohgushi, H., Yoshikawa, T., Sempuku, T., Tamai, S., Tabata, S. and Dohi, Y. (1999) Osteogenic phenotype expression of allogeneic rat marrow cells in porous hydroxyapatite ceramics. *J Bone Miner Res* 14:561–568.
- Boyer, L.A., Lee, T.I., Cole, M.F., Johnstone, S.E., Levine, S.S., Zucker, J.P., Guenther, M.G., Kumar, R.M., Murray, H.L., Jenner, R.G., Gifford, D.K., Melton, D.A., Jaenisch, R. and Young, R.A. (2005) Core transcriptional regulatory circuitry in human embryonic stem cells. *Cell* 122:947–956.
- D’Ippolito, G., Diabra, S., Howard, G.A., Menei, P., Roos, B.A. and Schiller, P.C. (2004) Marrow-isolated adult multilineage inducible (MIAMI) cells, a unique population of postnatal young and old human cells with extensive expansion and differentiation potential. *J Cell Sci* 117:2971–2981.
- El-Serag, H.B., Davilla, J.A., Petersen, N.J. and McGlynn, K.A. (2003) The continuing increase in the incidence of hepatocellular carcinoma in the United States. *Ann Intern Med* 139:817–823.
- Ikeda, E., Hirose, M., Kotobuki, N., Shimaoka, H., Tadokoro, M., Maeda, M., Hayashi, Y., Kirita, T. and Ohgushi, H. (2006) Osteogenic differentiation of human dental papilla mesenchymal cells. *Biochem Biophys Res Commun* 342:1257–1262.
- Iohara, K., Zheng, L., Ito, M., Tomokiyo, A., Matsushita, K. and Nakashima, M. (2006) Side population cells isolated from porcine dental pulp tissue with self-renewal and multipotency for dentinogenesis, chondrogenesis, adipogenesis, and neurogenesis. *Stem Cells* 24:2493–2503.

- Kogler, G., Sensken, S., Airey, J.A., Trapp, T., Muschen, M., Feldhahn, N., Liedtke, S., Sorq, R.V., Fischer, J., Rosenbaum, C., Greschat, S., Knipper, A., Bender, J., Deqistirci, O., Gao, J., Caplan, A.I., Colletti, E.J., Almeida-Porada, G., Muller, H.W., Zanjani, E. and Wernet, P. (2004) A new human somatic stem cell from placental cord blood with intrinsic pluripotent differentiation potential. *J Exp Med* 200:123–135.
- Lee, J.Y., Qu-Petersen, Z., Cao, B., Kimura, S., Jankowski, R., Cummins, J., Usas, A., Gates, C., Robbins, P., Wernig, A. and Huard, J. (2000) Clonal isolation of muscle-derived cells capable of enhancing muscle regeneration and bone healing. *J Cell Biol* 150:1085–1100.
- Miura, M., Gronthos, S., Zhao, M., Lu, B., Fisher, L.W., Robey, P.G. and Shi, S. (2003) SHED: stem cells from human exfoliated deciduous teeth. *Proc Natl Acad Sci USA* 100:5807–5812.
- Nagai, T., Ibata, K., Park, E.S., Kubota, M., Mikoshiba, K. and Miyawaki, A. (2002) A variant of yellow fluorescent protein with fast and efficient maturation for cell-biological applications. *Nat Biotechnol* 20:87–90.
- Ohgushi, H. and Caplan, A.I. (1999) Stem cell technology and bioceramics: from cell to gene engineering. *J Biomed Mater Res* 48:913–927.
- Ohgushi, H., Kotobuki, N., Funaoka, H., Hirose, M., Tanaka, Y. and Takakura, Y. (2005) Tissue engineered ceramic artificial joint—ex vivo osteogenic differentiation of patient mesenchymal cells on total ankle joints for treatment of osteoarthritis. *Biomaterials* 26:4654–4661.
- Oyagi, S., Hirose, M., Kojima, M., Okuyama, M., Kawase, M., Nakamura, T., Ohgushi, H. and Yagi, K. (2006) Therapeutic effect of transplanting HGF-treated bone marrow mesenchymal cells into CCl₄-injured rats. *J Hepatol* 44:742–748.
- Petersen, B.E., Bowen, W.C., Patrene, K.D., Mars, W.M., Sullivan, A.K., Boqq, S.S., Greenberger, J.S. and Goff, J.P. (1999) Bone marrow as a potential source of hepatic oval cells. *Science* 284:1168–1170.
- Reubinoff, B.E., Pera, M.F., Fong, C.Y., Trounson, A. and Bongso, A. (2000) Embryonic stem cell lines from human blastocysts: somatic differentiation in vitro. *Nat Biotechnol* 18:399–404.
- Sakaida, I., Terai, S., Yamamoto, N., Aoyama, K., Ishikawa, T., Nishina, H. and Okita, K. (2004) Transplantation of bone marrow cells reduces CCl₄-induced liver fibrosis in mice. *Hepatology* 40:1304–1311.
- Seo, B.M., Miura, M., Gronthos, S., Mark Bartold, P., Batouli, S., Brahim, J., Young, M., Gehron Robey, P., Wang, C.Y. and Shi, S. (2004) Investigation of multipotent postnatal stem cells from human periodontal ligament. *Lancet* 364:149–155.
- Seo, M.J., Suh, S.Y., Bae, Y.C. and Jung, J.S. (2005) Differentiation of human adipose stromal cells into hepatic lineage in vitro and in vivo. *Biochem Biophys Res Commun* 328:258–264.
- Tang, X.P., Zhang, M., Yang, X., Chen, L.M. and Zeng, Y. (2006) Differentiation of human umbilical cord blood stem cells into hepatocytes in vitro and in vivo. *World J Gastroenterol* 12:4014–4019.
- Theise, N.D., Badve, S., Saxena, R., Henegariu, O., Sell, S., Crawford, J.M. and Krause, D.S. (2000a) Derivation of hepatocytes from bone marrow cells in mice after radiation-induced myeloablation. *Hepatology* 31:235–240.
- Theise, N.D., Nimmakayal, M., Gardner, R., Illei, P.B., Morgan, G., Teperman, L., Henegariu, O. and Krause, D. (2000b) Liver from bone marrow in humans. *Hepatology* 32:11–16.
- Thomson, J.A., Itskovits-Eldor, J., Shapiro, S.S., Waknitz, M.A., Swiergiel, J.J., Marshall, V.S. and Jones, J.M. (1998) Embryonic stem cell lines derived from human blastocysts. *Science* 282:1145–1147.
- Toma, J.G., Akhavan, M., Karl, J.L., Fernandes, K.J., Barnabe-Heider, F., Sadikot, A., Kaplan, D.R. and Miller, F.D. (2001) Isolation of multipotent adult stem cells from the dermis of mammalian skin. *Nat Cell Biol* 3:778–784.
- Yen, B.L., Huang, H.I., Chien, C.C., Jui, H.Y., Ko, B.S., Yao, M., Shun, C.T., Yen, M.I., Lee, M.C. and Chen, Y.C. (2005) Isolation of multipotent cells from human term placenta. *Stem Cells* 23:3–9.
- Zipori, D. (2005) The stem state: plasticity is essential whereas self-renewal and hierarchy are optional. *Stem Cells* 23:719–726.
- Zuk, P.A., Zhu, M., Ashjian, P., De Ugarte, D.A., Huang, J.I., Mizuno, H., Alfonso, Z.C., Fraser, J.K., Benhaim, P. and Hedrick, M.H. (2002) Human adipose tissue is a source of multipotent stem cells. *Mol Biol Cell* 13:4279–4295.